Optimized Design and Implementation of a Micro-Sensor

A. M. Khodadadi Behtash, M. Maroufi, F. Barazandeh, and N. Sayyaf

***Abstract*—** In this paper a capacitive out of plane micro accelerometer is initially designed and implemented. To satisfy high sensitivity, low noise level and large full range capacitance change in 20g acceleration, two different optimization methods are used. The first method utilizes simple genetic algorithm (GA) and the second one uses nondominated sorting genetic algorithm (NSGA-II). Both of the methods use three constraint functions and five variable boundaries as hybrid read out circuit and fabrication limitations. Obtained results show good improvement in bandwidth and other performance parameters in comparison to the initial design parameters. Moreover, the results show that NSGA-II have a better flexibility in finding proper parameters and the obtained results can be varied according to the fabrication and readout circuit limitations.

***Keywords*—** Genetic algorithm, MEMS, NSGA-II, Optimization.

I. Introduction

MEMS acceleration sensors have been one of the most successful applications of MEMS technology which attract many attentions in design and optimization. These sensors are widely used in navigation and guidance applications, seismology, micro-gravity measurements and crash detection for air-bags. Resolution, sensitivity and noise level are some of the important performance parameters which the function of a micro accelerometer depends on them [1]. A good design requires proper selection between these parameters which have conflicting nature. The tuned parameters can be achieved by optimization methods. In many optimized sensors reported so far there are two approaches to reach an optimized design. The first approach is based on the exploitation of a single performance factor as a fitness function for the optimization procedure [2], [3]. In the second approach the optimization of a primary objective function (a combination of several secondary objective functions) is considered [4]. In these optimization methods each run of the optimization process results in a single optimized design regarding to the performance requirements.

The subject of this paper is the optimized modeling and implementation of a capacitive out of plane micro accelerometer. The optimization procedures are carried out by considering different objective functions. In order to reach an optimum design, two approaches are considered; in the first approach a simple constraint handling genetic algorithm (GA) is used. The aim of this optimization is to minimize the ratio of the mechanical noise to the sensitivity of the micro accelerometer by considering three constraints as the limiting factors. In the second approach a multiobjective genetic algorithm called NSGA-II [5] is employed to optimize three objective functions including: mechanical noise, sensitivity and full range capacitance change by the same constraints as the previous method.

A. M. Khodadadi Behtash, M. Maroufi, F. Barazandeh, and N. Sayyaf are with the Department of Mechanical Engineering, Amirkabir University of Technology (Polytechnic), Tehran, Iran (e-mails: amir.behtash@aut.ac.ir, fbarazandeh@aut.ac.ir, m.maroufi@aut.ac.ir, nima_sayyaf@yahoo.com) (corresponding author to provide phone: +982164543442; fax: +982166419736; e-mail: fbarazandeh@aut.ac.ir).

II. Sensor Design

Micromachined accelerometers are categorized into different groups due to their transduction mechanisms [1]. The proposed accelerometer uses differential capacitive mechanism to measure the displacement of the proof mass; the schematic of the proposed accelerometer is shown in Fig. 1. This accelerometer is a single axis out of plane sensor fabricated on 100 µm thick single crystal silicon (SCS) wafer by Reactive Ion Etching (RIE) process [6]. As shown in detailed view of this accelerometer, the proof mass is located between two similar caps fabricated from 500 µm single crystal silicon. The caps bonded to the frame from two opposite sides. A detailed view of the proof mass and its frame is shown in Fig. 2. The device uses four folded beams to suspend the proof mass between the cap plates. The fabricated mechanical element with its read out circuit is also shown in Fig. 3.

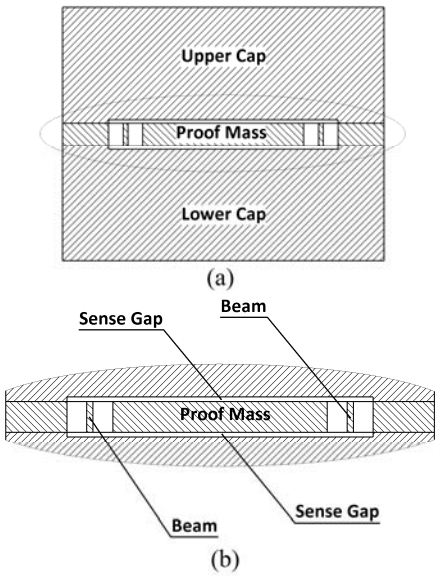

Fig. 1 (a) Schematic view of the proposed accelerometer, (b) Detailed view of the sensor parts

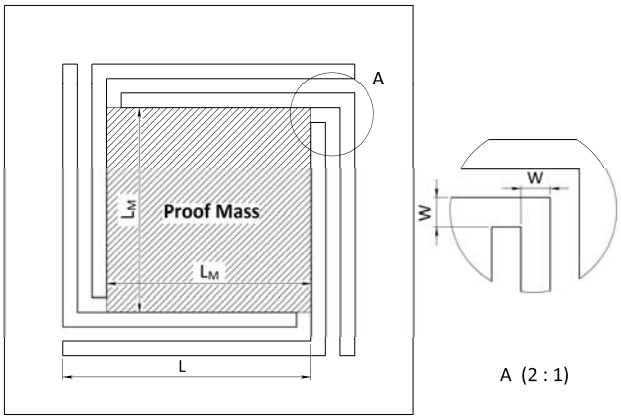

Fig. 2 Symbols for prototype sensor, L_M is the length of mass, W the width of beam and L is the length of beam

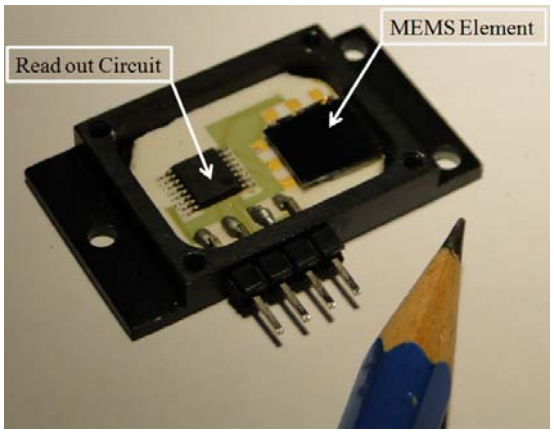

Fig. 3 Picture of the mechanical element and read out circuit

III. Theoretical Models

A. Mechanical Lumped Model

An accelerometer generally consists of a proof mass which is suspended against a fixed body. External acceleration displaces the mass relative to the support frame. The whole system can be modeled by a second order system which consists of an effective mass of M, an equivalent spring constant K and a damping factor of C, this model is shown in Fig. 4. The transfer function for mechanical part can be obtained by (1) [1].

$$\frac{Y(s)}{A(s)} = \frac{1}{S^2 + CS/M + K/M} \tag{1}$$

Where effective mass can be calculated as (2):

$$M = \left[\left(52L/35 + 200\times10^{-6}\right)W + L_M^2\right]t\rho \tag{2}$$

In this equation, ρ is the density of the silicon and t is the thickness of wafer. To consider the mass of the beam in this equation, it is assumed that the total mass of the beam is lumped on the beam's tip.

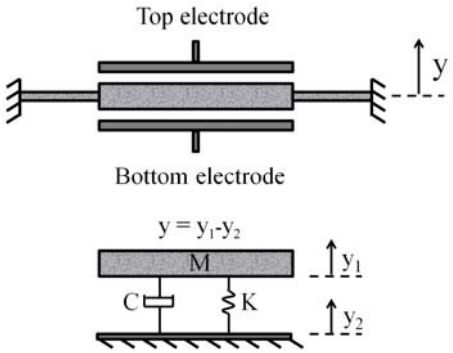

Fig. 4 Accelerometer lumped model

The proposed micro accelerometer consists of a proof mass connected to the frame by four folded beams. The beams suspend the proof mass against the inertial force (acceleration). The total spring constant K, stated in (3), is the sum of three spring constants including: K_{mech} as mechanical stiffness, K_{elec} as negative electrostatic stiffness and $K_{squeeze}$ as the elastic damping coefficient of the air [7].

$$K = K_{mech} + K_{elec} + K_{squeeze} \tag{3}$$

Mechanical stiffness can be calculated by (4), in which, E is the elastic modulus for the silicon beam.

$$K_{mech} = 4EWt^3 / L^3 \tag{4}$$

Also, the electrostatic stiffness can be calculated by the use of (5).

$$K_{elec} = -2\varepsilon_0 AV^2 / d_0^3 \tag{5}$$

Where A is the overlapping area of capacitance plates, V the rms excitation voltage applied to the capacitance plates by readout circuit and d_0 is the initial capacitance gap between the cap plates and the proof mass.

B. Squeeze Film Damping Model

In addition to the inertial force, the squeeze film damping effect is also present. The squeeze film effect is due to the trapped air between the proof mass and the stationary plates (upper and lower caps) [7].

In an oscillating MEMS structure, surrounding gas can profoundly affect the dynamic behavior of the system. This effect is due to the damping pressure acting on the moving plate. For a plate moving normally in front of a stationary one, damping pressure causes a resistive force against movement. This force consists of two components: viscous damping force and elastic damping force. The viscous damping is proportional to the velocity of the proof mass and the elastic damping is proportional to the proof mass displacement (as in (6)).

$$F_{squeeze} = -K_{squeeze} y - C_{squeeze} \dot{y} \tag{6}$$

Where $F_{squeeze}$ is squeeze film damping force acting on the proof mass, y is the displacement normal to the proof mass plate, and $\dot{y}$ is the first derivative of y which presents the plate's velocity.

Squeeze film damping in parallel plates can be defined by the use of linearized Reynold's equation [7]. For a rectangular plate it can be shown that the viscous and elastic damping coefficients are functions of squeeze number, σ and can be expressed as (7) and (8), respectively.

$$C_{squeeze} = \frac{64 P_a A \sigma}{\pi^6 d_0 \omega} \sum_{m,n\ odd} \left(m^2 + \left(n/\eta \right)^2 \right) ./ \left((mn)^2 \left\{ \left[m^2 + \left(n/\eta \right)^2 \right]^2 + \sigma^2 / \pi^4 \right\} \right) \tag{7}$$

$$K_{squeeze} = \frac{64 P_a A \sigma}{\pi^8 d_0} \cdot \sum_{m,n\ odd} \left((mn)^2 \left\{ \left[m^2 + \left(n/\eta \right)^2 \right]^2 + \sigma^2 / \pi^4 \right\} \right)^{-1} \tag{8}$$

Where P_a is the package pressure, d_0 the initial gap between parallel capacitance plates, ω the radial frequency of the plate oscillation, η the aspect ratio of the plate (ratio of length to width of the oscillating plate) which in this problem equals to 1, and A is the area of the plate (i.e., $A = L_M \times L_M$).

The squeeze number can be calculated by the use of (9):

$$\sigma = 12 \mu_{eff} \omega L_m^2 / \left(P_a d_0^2 \right) \tag{9}$$

In this equation μ_{eff} is the effective viscosity which can be modeled by (10).

$$\mu_{eff} = 1.79 \times 10^{-5} / \left(1 + 9.658 \left(\lambda / d_0 \right)^{1.159} \right) \tag{10}$$

Where, λ is the mean free pass of the air molecules. Regarding the above explanation, if the proof mass oscillates in a low frequency, the effect of elastic damping coefficient ($K_{squeeze}$) will be remarkable, but in low frequencies, this effect can be negligible in compare to mechanical spring constant (K_{mech}) and the dominating force would be the viscous damping force.

C. Natural Frequency Model

Natural frequency is one of the important parameters that can affect the mechanical specifications of an accelerometer. The first resonant mode of the designed accelerometer can be calculated as a function of total spring constant K, and the equivalent mass M, using spring-mass lumped parameter model:

$$f_n = \frac{1}{2\pi} \sqrt{\frac{K}{M}} \tag{11}$$

D. Sensor Noise Model

The total noise of a micro accelerometer consists of mechanical noise and electric readout circuit noise as stated in (12) [3].

$$Noise_{total} = \sqrt{Noise_{\text{mech}}^2 + Noise_{\text{elec}}^2} \tag{12}$$

Mechanical noise is an intrinsic noise due to damping and is called Brownian motion noise which results from the random collision of air molecules with the proof mass [8]. The Brownian noise depends on the surrounding gas temperature T, damping coefficient $C_{squeeze}$ (as in (7)) and the effective mass contributing in the oscillation M (as calculated in (2)). The acceleration noise resulted from Brownian noise is introduced in (13).

$$Noise_{mech} = \sqrt{\frac{4 K_B T C_{squeeze}}{M}} \left[\frac{m}{s^2} / \sqrt{Hz} \right] \tag{13}$$

In this equation K_B is the Boltzmann constant.

E. Capacitive Pick-off Model

According to the read out circuit specifications, the position of the proof mass is measured using changes in the capacitance on both sides of the proof mass (C_1-C_2), this value can be expressed as (14):

$$\Delta C_a = C_1 - C_2 = 2 \varepsilon_0 A y^2 / \left(d_0^2 - y^2 \right) \tag{14}$$

Where ΔC_a is the full range capacitance change in the applied acceleration a, and ε_0 is the permittivity of the dielectric (in this case air).

IV. Optimization

A. Simple Genetic Algorithm (GA)

Genetic algorithms (GAs) first introduced by Holland et al use the rules of natural species and eliminate unwanted individuals and transfer elite ones to the next generation via reproduction [9]. GA operates with a collection of individuals or chromosomes, called a population. Each individual can be a solution for the problem and is used to form new individuals by means of genetic operators.

Two operators are employed to generate new individuals from existing ones: crossover and mutation. The former is used as the major operator and the performance of a genetic

system is profoundly dependent on it, during this process two chromosomes (parents) are combined together and new chromosomes (offsprings) are formed. The latter one is the most important operator of GA and is used as the secondary operator to produce random changes in some chromosomes.

The next step is the selection step [9], and is applied to evaluate new individuals and to form new population by selecting the more fit individuals from the parent population and the offspring population.

In this study tournament selection method which employs pair wise selection is used. This operator satisfies three criteria to handle a constrained optimization problem [10]:

1- Any feasible solution is prior to infeasible one in the selection process.
2- Comparing two feasible solutions, the one with better objective function is desired.
3- Among two infeasible solutions, the bigger violation from constraints makes the chance of selection smaller.

It is needless to assign a penalty function to infeasible solutions in this method. The above steps are repeated till the stopping criterion (maximum number of generations) is met. In this study the maximum generations of 500, the population size of 20 are used. The crossover and mutation probabilities are set to be 0.75 and 0.05 respectively.

B. Multiobjective Nondominated Genetic Algorithm (NSGA-II)

Over the recent decades, a numbers of multiobjective evolutionary algorithms (MOEAs) are introduced. Multiobjective Genetic Algorithm (MOGA) by Fonseca and Fleming, Nondominated Sorting Genetic Algorithm (NSGA) by Srinivas and Deb, Niched Pareto Genetic Algorithm (NPGA) by Horn, Pareto-Archived Evolution Strategy (PAES) by Knowles and Strength Pareto Evolutionary Algorithm (SPEA) by Zitzler and Thiele are some of these proposed methods [11]. These kinds of algorithms are suitable for multiobjective optimization problems. NSGA-II, proposed by Deb et al [5], is one of the most efficient and well known multiobjective evolutionary algorithms which use nondominated sorting and crowding distance techniques to rank and select population fronts. The algorithm procedure is as follows:

1- The population initialization due to the problem range and constraints;
2- Sorting of individuals into different levels (fronts);
3- Assigning a nondomination number or a rank number (starting from 1 as the top and nondominated one) to each front and calculating the crowding distance.
4- Selecting operation using binary tournament selection method (picking out two solutions of the population and choosing the better one);
5- Employing crossover and mutation operators (offspring population Q_i is formed);
6- Forming new population R_i, combining random parent population P_i of size N and offspring population of the same size (i.e. $R_i=Q_i+P_i$);
7- Sorting the new population and assigning a rank number according to nondomination. Finally, a new population P_{i+1} will be obtained by removing the solutions overflowing N.

Repeating aforementioned procedure, a group of optimum solutions called Pareto optimal fronts will be achieved and decision maker can select each of them as a solution for the problem.

In this paper the population size of 200 and 1000 generations is used. The crossover and mutation probability rates are set on 0.75 and 0.05 respectively.

C. Optimization Functions

1) Single Objective Optimization

To achieve a sensor with high resolution, a low noise level as well as a high sensitivity is required [2]. The minimization of the ration introduced in (15) will satisfy both of these requirements simultaneously.

$$f = \sqrt{\frac{4K_B T C_{squeeze}}{M}\left[(\omega_n^2 - \omega^2) + \left(\frac{C_{squeeze}}{M}\omega\right)^2\right]} \qquad (15)$$

2) Multiobjective Optimization

The multiobjective optimization problem is established as follows:

- Maximization of the mechanical sensitivity derived from (1);

- Minimization of the Brownian noise in (13);

- Maximization of the full range capacitance change in 20g input acceleration presented in (14);

Each of these functions is taken as a distinct objective function in multiobjective procedure and a set of nondominated solutions has been obtained using NSGA-II.

Considering electrical read out circuit limits, fabrication process resolution and allowable space for the sensor system, a group of constraint functions and variable boundaries are introduced. These limiting values are shown in Table I. Since the values for viscous and elastic damping coefficients are functions of frequency ((7) and (8)), the constraint functions should be evaluated in each input acceleration frequency, so all of the optimizations including single and multiobjective,

TABLE I
CONSTRAINT FUNCTIONS AND VARIABLE BOUNDARIES USED IN OPTIMIZATION PROCEDURES

Constraints	Limit		Variables	Limit	
	Lower	Upper		Lower	Upper
BW (Hz)	300	600	L_M (mm)	3.3	4.9
C_0 (pF)	9.5	10.5	L (mm)	3.5	5.9
			W (μm)	50	100
ΔC_{20g} (pF)	$0.4C_0$	$0.6C_0$	P_a (KPa)	0.1	100
			d_0 (μm)	10	20

BW = Bandwidth, C_0 = Initial capacitance, ΔC_{20g} = Full range capacitance change, L_M = Length of mass, L = Length of beam, W = Width of beam, P_a = Package pressure, d_0 = Initial gap.

are carried out in three different working frequencies, 25, 125, 225 Hz in order to approximately sweep the whole working frequency range.

V. Results

Two optimization procedures are carried out by the use of single and multiobjective genetic algorithms. The aim of the first optimization is to minimize the ratio presented in the (15). Generally, three inequalities are defined as constraints for the first process. Using the variable boundaries developed in Table I, the optimization processes for three working frequencies will result in an optimized design for each frequency. Fig. 5 shows the convergence of the solution for the working frequency of 125Hz. The complete results for three above mentioned frequencies using the first optimization procedure are presented in Table II.

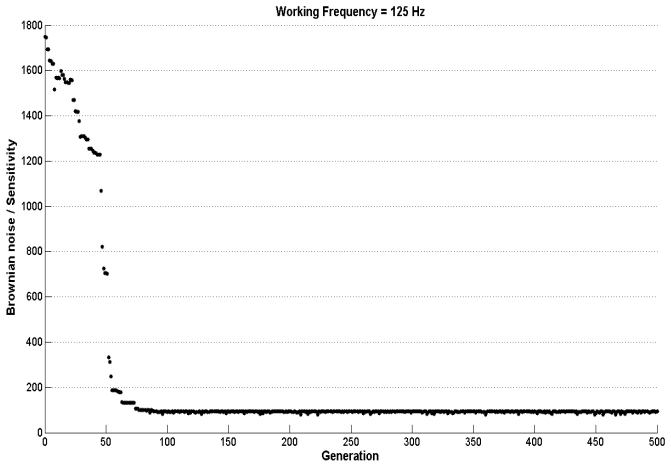

Fig. 5 Convergence to the solution in single objective optimization

Nondominated sorting genetic algorithm (NSGA-II) is also applied to the three objective functions introduced previously. In the NSGA-II process, the same constraints and boundaries are used as optimization requirements. In a multi-objective optimization problem generally there is not a single optimum solution that minimizes all of the objective functions simultaneously and instead several trade-off solutions (Pareto fronts) are usually selected as the optimum results [5]. The 3D and 2D plots of optimum fronts at the frequency of 125Hz are shown in Fig. 6, 7 and 8. To investigate the operation of the algorithm and compare the results with the single objective method, the extremum results for each of three objective functions are also presented in Table II.

VI. Discussion

As it is shown in Fig. 5, the simple genetic algorithm is successfully converged to an optimum value. In order to compare the results, the values of the performance functions in the initial design (before optimization) are also reported in Table II. The aim in single objective GA is to minimize the ratio of Brownian noise to sensitivity. A comparison between simple GA results and the results related to the design specifications before optimization shows that the results for sensitivity and Brownian noise are better in optimized designs. Additionally all of the optimized designs from GA, reported in Table II, have better bandwidths. The simple GA also results in a larger full range capacitance change in the full range operation of the sensor (i.e. in 20g input acceleration). The improvement achieved in capacitance change and also bandwidth is due to the constraints applied to the optimization process. The results depict that it is better to consider the package pressure around 100 Pa to result in a broader bandwidth and a lower noise level. If the cost of vacuum packaging is ignored this will be a good method to decrease the mechanical noise level and to increase the sensor's bandwidth [12]

In the optimization process with NSGA-II algorithm, all of the results (Table II) related to the extremum points (except the last design) have broader bandwidth than the first optimization process (GA). Major improvement is observed in the full range capacitance changes (about 151%) in compare to the initial design reported in this table for all results obtained by NSGA-II (except those for minimum Brownian noise). The results relating to the minimum Brownian noise show smaller improvement in full range capacitance changes (about 45%). Designs obtained by NSGA-II considering the minimum Brownian noise are not desirable because of the minimum detectable capacitance change limitations of the readout circuit. This small full range variation finally leads to reduce the sensor resolution. In spite of maximum bandwidth among the other designs, the results obtained from the Brownian noise extremums are not considered for further investigation. If the designs with the maximum full range capacitance changes are chosen, the Brownian noise level will be at its maximum level. This requires a trade-off between the designs with maximum full range capacitance change and minimum mechanical noise.

To find the appropriate solution between different designs proposed by NSGA-II, a compromise should be made between a lower noise and a larger full range capacitance change. For instance a full range capacitance change of about 6 pF is chosen to be appropriate regarding readout circuit specifications. According to Fig. 9 and 10 it will result in 2.75×10^{-6} $m/s^2/\sqrt{Hz}$ Brownian noise level and 2.70×10^{-8} $m/m/s^2$ sensitivity for the selected design working in the frequency of 125Hz. The complete result for the design variables and also the other two working frequencies is shown in Table III.

The results shown in Table III depict a better trade-off between the mechanical noise and the full range capacitance change in compare to results obtained from NSGA-II in Table II. Also, the optimization results in both of the methods show that the pressure near 100 Pa can cause better performance. Considering Table II and III it can be concluded that each optimization method (GA and NSGA-II) results in appropriate specifications for the micro accelerometer; however, it should be taken into account that the results from NSGA-II have better flexibility in order to find proper solutions.

TABLE II
RESULTS FOR SINGLE AND MULTIOBJECTIVE OPTIMIZATION AND INITIAL DESIGNS BEFORE OPTIMIZATION

Optimization type	Optimized specification	frequency (Hz)	Variables					Sensor specifications				
			L_M (μm)	L (μm)	W (μm)	d_0 (μm)	P_a (Pa)	$Noise_{mech}$ $\times 10^{-6}$ ($m/s^2/\sqrt{Hz}$)	$Sens\times 10^{-8}$ ($m/m/s^2$)	C_0 (pF)	ΔC_{20g} (pF)	BW (Hz)
Initial design		25	4410	5160	90	17	10^5	2122.2	1.04	10.12	2.51	118
Single objective	$Noise_{mech}$ / Sens	25	4871.1	5871.1	59.9	20.0	100.0	2.68	2.83	10.50	6.30	378.74
		125	4857.5	5857.5	59.1	20.0	100.0	2.68	2.83	10.44	6.26	378.74
		225	4679.1	5679.1	50.0	20.0	100.0	2.69	2.82	9.69	5.79	379.22
Multi objective	$Noise_{mech}$	25	4638.0	5623.0	99.8	20.0	100.1	2.64	1.37	9.52	2.61	543.44
		125	4633.7	5633.7	100.0	20.0	100.0	2.62	1.38	9.50	2.61	542.74
		225	4871.2	5871.2	100.0	20.0	100.0	2.58	1.75	10.50	3.64	485.82
	ΔC_{20g}	25	4736.7	5631.6	52.7	18.9	110.7	3.00	2.67	10.50	6.30	389.43
		125	4757.3	5740.9	56.0	19.1	105.2	2.87	2.71	10.50	6.29	387.95
		225	4832.4	5820.2	58.3	19.7	110.8	2.81	2.85	10.50	6.30	381.76
	Sensitivity	25	4734.4	5724.9	53.1	20.0	101.3	2.71	2.78	9.92	5.85	381.64
		125	4789.2	5786.4	55.8	20.0	100.0	2.68	2.83	10.21	6.11	380.45
		225	4840.4	5840.1	58.3	20.0	100.2	2.62	2.91	10.37	6.20	379.18

Noisemech = Brownian noise, Sens = Mechanical sensitivity

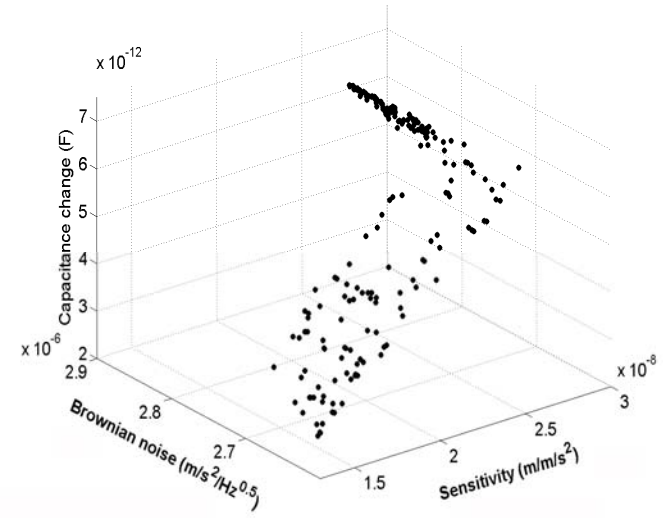

Fig. 6 Pareto optimal fronts for sensitivity, capacitance change and Brownian noise in 125Hz as working frequency

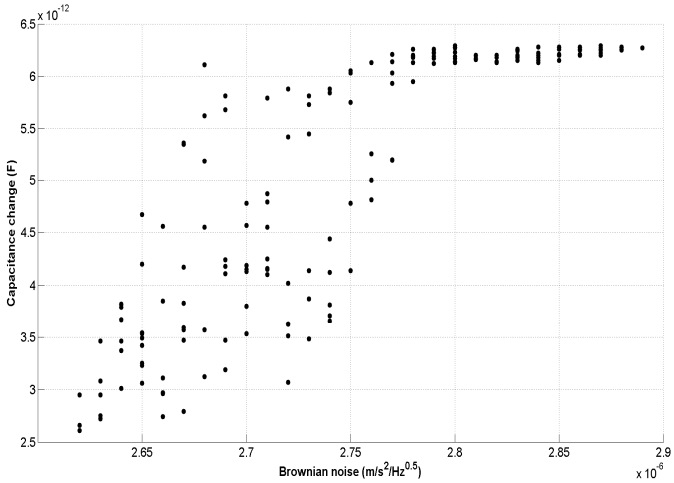

Fig. 7 Pareto front for Brownian noise vs. capacitance change in 125Hz as working frequency

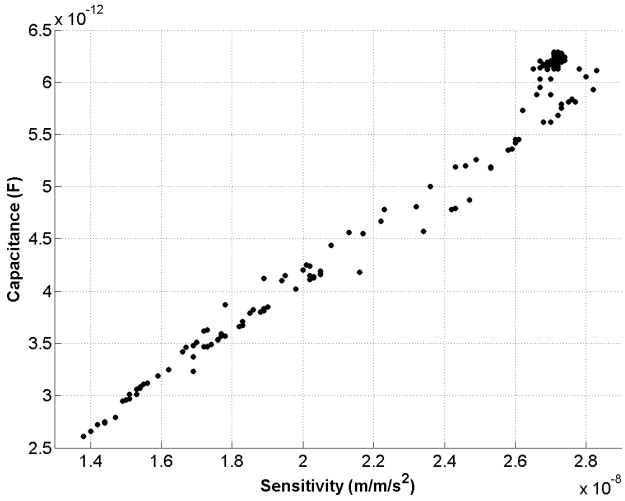

Fig. 8 Pareto front for sensitivity vs. capacitance change in 125Hz as working frequency

It is evident from Table III that the bandwidth values for three designs with different frequencies have the maximum difference of 0.45%, so with a good approximation they can be assumed the same. Because of the bigger initial capacitance, sensitivity and also lower Brownian noise of the third design in this table, it is selected as the final design achieved from NSGA-II method for the fabrication. Moreover for the first optimization method, regarding Table II, the results for the bandwidth show the maximum difference of 0.13% and they can be assumed the same. The first design of GA method (Table II) is selected as the final design achieved from GA for the fabrication (because of its bigger initial capacitance and also its bigger full range capacitance change). The selected designs from each of the two optimization methods are shown in Table IV. The frequency response diagrams for these two selected designs and the Initial design (before optimization) are depicted in Fig. 9. As this figure shows, the bandwidth for the two selected designs from GA and NSGA-II are broader than the Initial design before

TABLE III
RESULTS FOR THE PROPOSED DESIGN FROM NSGA-II FOR FULL RANGE CAPACITANCE CHANGE OF ABOUT 6 PF

frequency (Hz)	Variables					Sensor specifications				
	L_M (μm)	L (μm)	W (μm)	d_0 (μm)	P_a (Pa)	$Noise_{mech}$ $\times 10^{-6}$ ($m/s^2/\sqrt{Hz}$)	Sens $\times 10^{-8}$ ($m/m/s^2$)	C_0 (pF)	ΔC (pF)	BW (Hz)
25	4732.0	5621.3	52.5	19.3	100.2	2.79	2.66	10.27	6.00	390.12
125	4750.7	5712.1	55.36	19.3	100.2	2.75	2.70	10.35	6.03	389.32
225	4831.3	5818.3	60.3	19.7	100.0	2.65	2.77	10.49	6.01	388.36

TABLE IV
FINAL DESIGNS FROM GA AND NSGA-II METHODS IN COMPARE TO INITIAL DESIGN (BEFORE OPTIMIZATION)

Design type	Variables					Sensor specifications				
	L_M (μm)	L (μm)	W (μm)	d_0 (μm)	P_a (Pa)	$Noise_{mech}$ $\times 10^{-6}$ ($m/s^2/\sqrt{Hz}$)	Sens$\times 10^{-8}$ ($m/m/s^2$)	C_0 (pF)	ΔC (pF)	BW (Hz)
Initial design	4410	5160	90	17	10^5	2122.2	1.04	10.12	2.51	118
GA	4871.1	5871.1	59.9	20.0	100.0	2.68	2.83	10.50	6.30	378.74
NSGA-II	4831.3	5818.3	60.3	19.7	100.0	2.65	2.77	10.49	6.01	388.36

optimization. Considering results in Table IV it can be expressed that the selected design from GA method shows increment of about 172%, 151% and 221% in sensitivity, full range capacitance change and band width respectively. Also the selected design from NSGA-II method shows increment of about 166%, 139% and 229% in sensitivity, full range capacitance change and band width respectively.

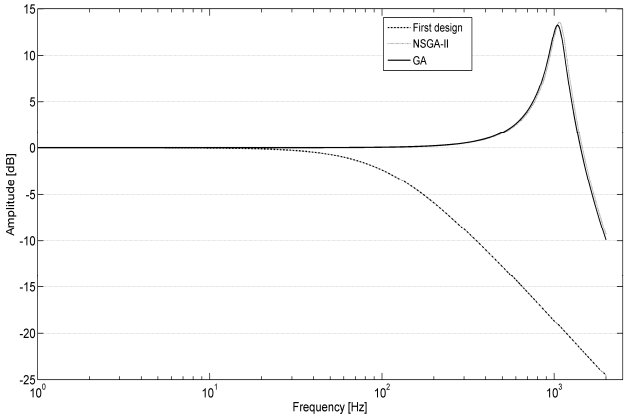

Fig. 9 Frequency response for initial design before optimization, design from GA and design obtained from NSGA-II

VII. CONCLUSION

An out of plane capacitive micro accelerometer is designed and implemented. In order to improve the performance parameters of the sensor, geometrical dimensions and also packaging pressure of the sensor are optimized using two optimization methods: simple genetic algorithm (GA) and nondominated sorting genetic algorithm (NSGA-II). Most of the constraints and variable boundaries are provided by the fabrication and readout circuit limitations. Both simple GA and NSGA-II algorithms show good convergence to the optimum results and also they will converge to the pressures approximately near 100 Pa as the packaging appropriate pressure. Simple GA algorithm converges to a specific solution that will satisfy the constraints but any change in the design specifications requires a new optimization process, which will be time consuming. On the contrary, the multi-objective algorithm (NSGA-II) provides a set of optimum results and the designer may select the most appropriate one. Furthermore the trade-off selection between lots of designs is a big advantage of a multi objective approach to a single objective one. Considering these optimization methods, two optimum designs are selected according to mechanical, electrical and fabrication process limits. These designs show a great improvement in performance parameters of the micro accelerometer in compare to the initial design (before optimization).

REFERENCES

[1] N. Yazdi, F. Ayazi, K. Najafi, "Micromachined inertial sensors," *Proceedings of the IEEE,* vol. 86, No. 8, pp. 1640-1659, 1998.

[2] J. Chae, H. Kulah, K. Najafi, "A CMOS compatible high aspect ratio silicon-on-glass in-plane micro-accelerometer," *Micromechanics and Microengineering J.,* Vol. 15, pp. 336–345, 2005.

[3] P. Monajemi, F. Ayazi, "Design optimization and implementation of a microgravity capacitive HARPSS accelerometer", *IEEE Sensors Journal J.*, vol. 6, No. 1, pp. 39-46, 2006.

[4] J. K. Coultate, C. H. J. Fox, S. McWilliam, A. R. Malvern, "Application of optimal and robust design methods to a MEMS accelerometer," *Sensors and Actuators A J.,* 2007.

[5] K. Deb, A. Pratap, S. Agarwal, T. Meyarivan, "A fast and elitist multiobjective genetic algorithm: NSGA-II", *IEEE Transactions on evolutionary computation*, vol.6, No.2, pp. 182-197, 2002.

[6] IW. Rangelow, H. Loschner, "Reactive ion etching for microelectrical mechanical system fabrication" *Vacuum Science & Technology B: Microelectronics and Nanometer Structures J.*, vol. 13, No. 6, pp. 2394-2399, 1995.

[7] M. Bao, H. Yang, "Squeeze film air damping in MEMS," *Sensors and Actuators A*, vol. 136, pp. 3-27, 2007.

[8] SD. Senturia, "Microsystem design," MA: Kluwer Academic Publishers, 2001.

[9] M. Gen, R. Cheng, "Genetic algorithms and engineering optimization," New York: John Wiley & Sons Inc, 2000.

[10] K. Deb, "An efficient constraint handling method for genetic algorithms," *Computer Methods in Applied Mechanics and Engineering*, vol. 186, No. 2-4, pp. 311-338, 2000.

[11] A. Konak, DW. Coit, AE. Smith, "Multi-objective optimization using genetic algorithms: a tutorial," *Reliability Engineering and System Safety*, vol. 91, pp. 992-1007, 2006.

[12] J. Chae, H. Kulah, K. Najafi, "An in-plane high-sensitivity, low-noise micro-g silicon accelerometer with CMOS readout circuitry," *Microelectromechanical systems J*., vol. 13, No. 4, 2004.